

Scientific Research Report

Comprehensive Analysis of Orthodontic Treatment Effects on the Oral Microbiome, Metabolome, and Associated Health Indicators

Qin Xie^a, Duo Li^a, Chengyan Ren^b, Hao Liang^c, Ge Shi^c, Weihui Chen^{b*}^a Department of Stomatology, Fujian Medical University Union Hospital, Fuzhou, China.^b Department of Oral and Maxillofacial Surgery, Fujian Medical University Union Hospital, Fuzhou, China^c School of stomatology, Fujian Medical University, Fuzhou, China

ARTICLE INFO

Article history:

Received 24 October 2024

Received in revised form

23 January 2025

Accepted 19 February 2025

Available online xxx

Keywords:

Orthodontic treatment

Microbiome

Metabolome

Oral hygiene indicators

Machine learning

ABSTRACT

Introduction and Aims: Effects of orthodontic treatments on oral health, particularly on the microbiome and metabolome, are not well understood, and this study aims to clarify these influences using multi-omics approaches.

Methods: We used 16S rRNA sequencing to analyze oral microbiota and untargeted metabolomics for metabolic profiling, comparing clear aligners (CAs) and fixed appliances (FAs) in healthy and unhealthy oral environments.

Results: We found CAs significantly improve oral health markers—including reduced plaque accumulation, enamel demineralization, microbiome alpha diversity, and microbial heterogeneity, especially in unhealthy oral environments. Orthodontic treatment type and overall oral health status significantly altered the oral microbiota structure and metabolite composition. Notably, the effect of orthodontic methods was more pronounced on metabolome than on microbiome. There's a strong link between changes in oral microbiome, health status, and hygiene habits. For example, *Prevotella* and *Treponema* were linked to poor oral health indicators, whereas *Rothia*, *Granulicatella*, and *Streptococcus* were associated with good oral hygiene indicators. Machine learning analysis identified 13 key metabolites, including cholyarginine, alpha-CEHC glucuronide, 2-hydroxypentanoic acid, Cer (d17:1/6 keto-PGF1alpha), and LysoPE (15:0/0:0), which were associated with inflammatory responses and served as predictive markers for poor oral health. These metabolites were closely correlated with specific microbial species enriched in oral environment, including *Rothia*, *Prevotella*, and *Anaeroglobus*, suggesting their potential as biomarkers for oral health monitoring. KEGG enrichment revealed differential metabolites were significantly enriched in alkaloid biosynthesis pathways, particularly map01064, which is crucial for polyamine synthesis related to bacterial activities.

Conclusion: CAs significantly improve oral health markers, particularly affecting the metabolome more than the microbiome, with key metabolites and microbial species serving as potential biomarkers for oral health monitoring.

Clinical Relevance: This study provides comprehensive insights into interactions among orthodontic treatments, oral health status, microbial, and metabolic dynamics, offering foundation for developing personalized strategies in oral health management and orthodontic care.

© 2025 The Authors. Published by Elsevier Inc. on behalf of FDI World Dental Federation.

This is an open access article under the CC BY-NC-ND license

[\(http://creativecommons.org/licenses/by-nc-nd/4.0/\)](http://creativecommons.org/licenses/by-nc-nd/4.0/)

Introduction

Oral health plays a critical role in overall health, with poor oral hygiene linked to various systemic diseases, including cardiovascular and metabolic disorders.¹⁻³ Although orthodontic

* Corresponding author. Department of Oral and Maxillofacial Surgery, Fujian Medical University Union Hospital, Fuzhou, China.

E-mail address: whchen@fjmu.edu.cn (W. Chen).

<https://doi.org/10.1016/j.identj.2025.02.014>

0020-6539/© 2025 The Authors. Published by Elsevier Inc. on behalf of FDI World Dental Federation. This is an open access article under the CC BY-NC-ND license (<http://creativecommons.org/licenses/by-nc-nd/4.0/>)

treatments, particularly clear aligners (CAs) and fixed appliances (FAs), are widely used to correct malocclusions, they can also influence oral health outcomes, including the risk of enamel demineralization, plaque accumulation, and dental caries.^{4,5} Understanding these complex relationships is vital to optimizing orthodontic treatments and promoting long-term oral health.⁶

The type of orthodontic treatment, combined with the patient's oral hygiene practices and overall health, remarkably affects the oral microbiota and chemical environment within the mouth.⁷ Recent studies have shown that CA treatments do not considerably alter the subgingival microbiome composition but can attract a unique microbial community with low diversity at the tray level while maintaining overall periodontal health.⁸ Furthermore, longitudinal comparisons of fixed orthodontic appliances and CAs revealed substantial differences in plaque accumulation and gingival health, with CAs associated with better oral health indices and less microbial diversity changes than FAs.⁵ While most studies focused on microbial aspects, understanding metabolic changes is crucial for early disease detection, microbiome interactions, and personalized treatments, with key biomarkers potentially enhancing preventive measures and therapeutic strategies for improved oral health management.⁹ In particular, no reports exist on the effect of different orthodontic treatments on the oral microbiome under unhealthy oral conditions, which help understand potential oral health issues that may arise during orthodontic treatment.

Our study aims to address the existing knowledge gap by evaluating how different orthodontic treatments and various oral health conditions, particularly those that are unhealthy, affect the oral microbiome and metabolome and key oral health indicators. The findings reveal that in an unhealthy oral environment, CAs significantly improve key oral health indicators compared with FAs. Moreover, changes in clinical factors are strongly correlated with variations in the oral microbiome and metabolome. By applying a machine learning approach based on the LASSO algorithm to select key features,¹⁰ 13 significant metabolites were identified as key predictors of poor oral health, with several of these metabolites showing notable associations with specific core oral microbial species. These insights could help develop more effective interventions to mitigate the negative effects of orthodontic treatments on oral health, enhance patient outcomes, improve overall oral health management and lay a foundation for future research into the complex regulatory mechanisms between microbes and metabolites following orthodontic treatment.

Materials and methods

Experimental design and sampling

The study was approved by the Ethics Committee of Union Hospital, affiliated with Fujian Medical University. Written informed consent was obtained from the legal parents or guardians of all participants prior to the start of the study. This cross-sectional study was conducted in accordance with the STROBE guidelines. From November 23, 2023, to December 30, 2023, adolescents ($n = 61$) receiving treatment in the Department of Orthodontics at Fujian Medical University Union Hospital were recruited. The participants were divided

into 6 groups: 10 volunteers with good oral hygiene who were not undergoing orthodontic treatment (CKH), 10 volunteers with poor oral hygiene who were not undergoing orthodontic treatment (CKU), 10 patients undergoing clear aligner therapy (angelalign®) with good oral hygiene (CAH), 10 patients undergoing clear aligner (angelalign®) therapy with poor oral hygiene (CAU), 10 patients undergoing fixed orthodontic (Ormco®) treatment with good oral hygiene (FAH), and 11 patients undergoing fixed orthodontic (Ormco®) treatment with poor oral hygiene (FAU). In this study, a plaque index of 0, 1, or 2 was classified as good oral hygiene, while a plaque index of 3, 4, or 5 was classified as poor oral hygiene. Plaque detection was performed by a single, well-trained periodontist who independently assessed the plaque index of patients and ensured consistency in the evaluations.¹¹

Patients were selected based on the following inclusion criteria: in the clear aligner group, 20 patients changed their aligners (angelalign®) every 7–10 days and had been undergoing clear aligner therapy for over a year while in the fixed appliance group, patients were treated with fixed orthodontic appliances (Ormco®) for more than a year. Exclusion criteria included patients with periodontal disease, systemic diseases, or those who had received antibiotic treatment in the past 3 months. Data on the enrolled participants' 4 general demographic indicators (gender, age, height, and weight), 3 lifestyle-related factors (daily brushing frequency, use of electric toothbrushes, and use of mouthwash), and 3 oral health indicators (plaque index, enamel demineralization, and number of decayed teeth) were collected via questionnaire (Table 1). To minimize circadian rhythm disruptions, sample collection was scheduled between 8:00 and 9:00 a.m. Participants were instructed to avoid eating or drinking prior to plaque collection and to rest for at least 20 minutes before the sampling. Plaque was collected from the gingival margins of teeth 16, 11, 26, 36, 31, and 46 using sterile cotton swabs, carefully scraping the plaque from the tooth surface. The collected samples were temporarily stored in liquid nitrogen, then kept in a -80°C freezer, and prepared for 16Sv34 amplicon sequencing and untargeted metabolomics analysis.

DNA extraction of swab microbiome and amplicon sequencing

Total microbial genomic DNA was extracted from 61 dental plaque swab samples using the FastPure Stool DNA Isolation Kit (MJYH, Shanghai, China), following the manufacturer's protocol. DNA quality and concentration were assessed by 1.0% agarose gel electrophoresis and a NanoDrop® ND-2000 spectrophotometer (Thermo Scientific, USA), and the DNA samples were stored at -80°C until further analysis. The hypervariable V3–V4 region of the bacterial 16S rRNA gene was amplified using the primer pairs 338F (5'-ACTCCTACGG-GAGGCAGCAG-3') and 806R (5'-GGACTACHVGGGTWCT-TAAT-3')¹ on a T100 Thermal Cycler (Bio-Rad, USA). The PCR reaction mixture contained 4 μL of $5\times$ Fast Pfu buffer, 2 μL of 2.5 mM dNTPs, 0.8 μL of each primer (5 μM), 0.4 μL of Fast Pfu polymerase, 10 ng of template DNA, and ddH₂O to a final volume of 20 μL . The PCR cycling conditions were as follows: initial denaturation at 95°C for 3 minutes, followed by 27 cycles of denaturation at 95°C for 30 seconds, annealing at 55°C for 30 seconds, and extension at 72°C for 45 seconds, with a final

Table 1 – Patient characteristics based on the patient's oral plaque control condition and orthodontic treatment methods.

Variable	Overall (N = 61*)	CKH (N = 10*)	CKU (N = 10*)	CAH (N = 10*)	CAU (N = 10*)	FAH (N = 10*)	FAU (N = 11*)	P-value
Gender								.500
Female	36 (59%)	5 (50%)	4 (40%)	8 (80%)	5 (50%)	7 (70%)	7 (64%)	
Male	25 (41%)	5 (50%)	6 (60%)	2 (20%)	5 (50%)	3 (30%)	4 (36%)	
Age	23 (14, 28)	25 (23, 29)	29 (21, 40)	28 (23, 29)	15 (12, 21)	25 (20, 28)	13 (13, 16)	<.001
Height	163 (156, 170)	166 (161, 170)	162 (155, 171)	164 (160, 166)	162 (156, 172)	167 (160, 170)	156 (150, 170)	.600
Weight	55 (50, 70)	64 (52, 75)	65 (53, 70)	55 (52, 76)	54 (47, 67)	58 (47, 67)	50 (44, 58)	.110
Daily brushing frequency								.005
1	10 (16%)	0 (0%)	5 (50%)	0 (0%)	2 (20%)	0 (0%)	3 (27%)	
2	38 (62%)	8 (80%)	5 (50%)	6 (60%)	6 (60%)	6 (60%)	7 (64%)	
3	10 (16%)	2 (20%)	0 (0%)	3 (30%)	2 (20%)	2 (20%)	1 (9.1%)	
4	1 (1.6%)	0 (0%)	0 (0%)	0 (0%)	0 (0%)	1 (10%)	0 (0%)	
5	2 (3.3%)	0 (0%)	0 (0%)	1 (10%)	0 (0%)	1 (10%)	0 (0%)	
Plaque index								<.001
0	5 (8.2%)	5 (50%)	0 (0%)	0 (0%)	0 (0%)	0 (0%)	0 (0%)	
1	16 (26%)	5 (50%)	0 (0%)	3 (30%)	0 (0%)	8 (80%)	0 (0%)	
2	9 (15%)	0 (0%)	0 (0%)	7 (70%)	0 (0%)	2 (20%)	0 (0%)	
3	14 (23%)	0 (0%)	8 (80%)	0 (0%)	5 (50%)	0 (0%)	1 (9.1%)	
4	16 (26%)	0 (0%)	2 (20%)	0 (0%)	5 (50%)	0 (0%)	9 (82%)	
5	1 (1.6%)	0 (0%)	0 (0%)	0 (0%)	0 (0%)	0 (0%)	1 (9.1%)	
Enamel demineralization								<.001
No	24 (39%)	10 (100%)	4 (40%)	5 (50%)	0 (0%)	3 (30%)	2 (18%)	
Yes	37 (61%)	0 (0%)	6 (60%)	5 (50%)	10 (100%)	7 (70%)	9 (82%)	
Decayed teeth								.002
No	26 (43%)	10 (100%)	4 (40%)	5 (50%)	3 (30%)	2 (20%)	2 (18%)	
Yes	35 (57%)	0 (0%)	6 (60%)	5 (50%)	7 (70%)	8 (80%)	9 (82%)	
Use of electric Toothbrush								.020
No	40 (66%)	8 (80%)	8 (80%)	4 (40%)	3 (30%)	7 (70%)	10 (91%)	
Yes	21 (34%)	2 (20%)	2 (20%)	6 (60%)	7 (70%)	3 (30%)	1 (9.1%)	
Use of mouthwash								.014
No	45 (74%)	8 (80%)	10 (100%)	4 (40%)	8 (80%)	5 (50%)	10 (91%)	
Yes	16 (26%)	2 (20%)	0 (0%)	6 (60%)	2 (20%)	5 (50%)	1 (9.1%)	

* n(%); Median (Q1,Q3).

† Fisher's exact test; Kruskal-Wallis rank sum test.

extension at 72 °C for 10 minutes and a hold at 4 °C. All samples were amplified in triplicate. PCR products were extracted from a 2% agarose gel, purified, and quantified using a Synergy HTX microplate reader (Biotek, USA). Purified amplicons were pooled in equimolar amounts and sequenced using paired-end sequencing on an Illumina NextSeq 2000 PE300 platform (Illumina, San Diego, USA) following standard protocols by Majorbio Bio-Pharm Technology Co. Ltd. (Shanghai, China).

Metabolite extraction and LC-MS/MS analysis

A 50 mg solid sample was placed into a 2 mL centrifuge tube, along with a 6 mm diameter grinding bead. To extract metabolites, 400 µL of extraction solution (methanol = 4:1, v/v) containing 0.02 mg/mL of the internal standard (L-2-chlorophenylalanine) was added. Samples were ground using a Wonbio-96c frozen tissue grinder (Shanghai Wanbo Biotechnology Co., Ltd.) for 6 minutes at –10 °C and 50 Hz, followed by low-temperature ultrasonic extraction at 5 °C and 40 kHz for 30 minutes. After incubation at –20 °C for 30 minutes, the samples were centrifuged at 13,000 g for 15

minutes at 4 °C, and the supernatant was transferred to an injection vial for LC-MS/MS analysis. As part of the system conditioning and quality control process, a pooled quality control (QC) sample was prepared by combining equal volumes of all individual samples. The QC samples were processed and tested under the same conditions as the analytical samples. These QC samples, representing the entire sample set, were injected at regular intervals (every 5-15 samples) to monitor the stability and consistency of the analysis.

LC-MS/MS analysis was performed on a Thermo UHPLC-Q Exactive HF-X system equipped with an ACQUITY HSS T3 column (100 mm × 2.1 mm i.d., 1.8 µm; Waters, USA) at Majorbio Bio-Pharm Technology Co. Ltd. (Shanghai, China). The mobile phases consisted of 0.1% formic acid in water (95:5, v/v) (solvent A) and 0.1% formic acid in acetonitrile: isopropanol (47.5:47.5:5, v/v) (solvent B). For positive ion mode, the separation gradient was as follows: 0-3 min, mobile phase B increased from 0% to 20%; 3-4.5 min, B increased from 20% to 35%; 4.5-5 min, B increased from 35% to 100%; 5-6.3 min, B was maintained at 100%; 6.3-6.4 min, B decreased from 100% to 0%; 6.4-8 min, B was held at 0%. For negative ion mode, the

gradient was as follows: 0–1.5 min, B increased from 0% to 5%; 1.5–2 min, B increased from 5% to 10%; 2–4.5 min, B increased from 10% to 30%; 4.5–5 min, B increased from 30% to 100%; 5–6.3 min, B was maintained at 100%; 6.3–6.4 min, B decreased from 100% to 0%; 6.4–8 min, B was held at 0%. The flow rate was 0.40 mL/min, and the column temperature was maintained at 40 °C. Mass spectrometric data were collected on a Thermo UHPLC-Q Exactive HF-X mass spectrometer equipped with an electrospray ionization (ESI) source, operating in both positive and negative ion modes. Optimal conditions were as follows: source temperature of 425 °C, sheath gas flow rate of 50 arb, auxiliary gas flow rate of 13 arb, and ion spray voltage of –3500 V in negative mode and 3500 V in positive mode. Normalized collision energy was set to 20–40–60 V rolling for MS/MS. Full MS resolution was 60,000, and MS/MS resolution was 7,500. Data acquisition was performed in Data Dependent Acquisition (DDA) mode, with detection over a mass range of 70–1050 m/z.

Bioinformatics analysis

After demultiplexing, the sequences were quality filtered using fastp (v0.19.6)¹² and merged with FLASH (v1.2.11).¹³ High-quality sequences were then denoised using the DADA2¹⁴ (or Deblur) plugin in the QIIME2 (version 2020.2)¹⁵ pipeline with recommended parameters, achieving single nucleotide resolution based on error profiles within samples. The denoised sequences generated by DADA2 (or Deblur) are referred to as amplicon sequence variants (ASVs). To minimize the effects of sequencing depth on alpha and beta diversity measures, the number of sequences from each sample was rarefied to 20,000, which still provided an average Good's coverage of 97.90%. Taxonomic assignment of ASVs was performed using the Naive Bayes (or Vsearch, or BLAST) consensus taxonomy classifier implemented in QIIME2, referencing the SILVA 16S rRNA database (v138).¹⁶ Using the ASV data, alpha diversity indices, including Ace and the Shannon index, were calculated with Mothur v1.30.2.

LC/MS raw data were preprocessed using Progenesis QI software (Waters Corporation, Milford, USA), resulting in the export of a 3-dimensional data matrix in CSV format. This matrix contained sample information, metabolite names, and mass spectral response intensities. Internal standard peaks, along with any known false-positive peaks (such as noise, column bleed, and derivatized reagent peaks), were removed from the data matrix, which was then de-reduced and pooled. Metabolites were identified by searching major databases, including HMDB (<http://www.hmdb.ca/>), Metlin (<https://metlin.scripps.edu/>), and the Majorbio Database.¹⁷

Statistical analysis

Clinical indicators were analyzed using the R gtsummary package to generate baseline tables. The Wilcoxon rank-sum test was applied for testing differences in continuous variables, while Pearson's Chi-squared test was used for non-continuous variables. Using the sklearn package, we constructed Lasso, Random Forest, and SVM models for the metabolites, and performed subcluster clustering using hierarchical clustering (based on Euclidean distance). The pheatmap package

was used to create heatmaps. We conducted a Mantel test between genus-level species abundance tables and the key metabolic features identified by the machine learning models (based on Bray-Curtis distance) using the vegan package (2.4.3) and the sgchart plugin. RDA and VPA analysis were performed using the vegan package (version 2.4.3) in R. Linear regression was performed using the lm function in R. The association networks between the microbiome and metabolome ($|r| > 0.6$, $P < .05$), as well as the networks between key microbes and metabolites, were visualized using Cytoscape v3.10.2. Hub genes and network were performed using CytoHubba.¹⁸

Result

CAs improve oral health more than FAs, especially in unhealthy environments

We collected data on 4 general demographic indicators (gender, age, height, and weight), 3 lifestyle-related factors (daily brushing frequency, use of electric toothbrushes, and use of mouthwash), and 3 oral health indicators (plaque index, enamel demineralization, and number of decayed teeth) to compare variations in orthodontic outcomes across populations with different orthodontic methods and oral health conditions. Firstly, comparing groups based solely on oral health status (Supplemental table 1), there were no significant differences in general demographic indicators, with the exception of age (P -value = .002). However, individuals in the oral health group demonstrated a significantly higher daily brushing frequency, greater use of mouthwash, lower plaque index, lower incidence of enamel demineralization, and lower proportion of decayed teeth. Notably, there was no significant difference in the use of electric toothbrushes between the 2 groups. In conclusion, oral health is strongly associated with lifestyle-related factors and is clearly reflected by key oral health indicators.

Subsequently, upon further subdividing the groups based on the influence of orthodontic methods, comparisons were made within healthy oral environments (groups CKH, CAH, and FAH) or unhealthy oral environments (groups CKU, CAU, and FAU). Across healthy (Supplemental Table 2) and unhealthy groups (Supplemental Table 3), those with FAs and CAs showed a significant increase in the plaque index. Furthermore, the FA group had a higher plaque index, a greater proportion of enamel demineralization, and a higher rate of decayed teeth than the CA group. This finding suggests that wearing braces increases the risk of oral health deterioration, with CAs offering a relative improvement in oral health over FAs.

Oral health and orthodontic treatments significantly reshape oral microbiota and enrich specific bacterial taxa

We conducted the amplicon sequencing of the V3–V4 region, generating a total of 4,049,325 clean reads and identifying 20,684 amplicon sequencing variants (ASVs) to evaluate the effect of various orthodontic treatments and oral health conditions on the oral microbiota. An unhealthy oral

environment significantly increased the alpha diversity of the oral microbiota, including the Shannon and ACE indices (Figures S1A, B). Beta diversity analysis using PLS-DA also revealed a clear separation between unhealthy and healthy oral environments (Supplemental Figure 1C), indicating distinct microbial community structures between the 2 groups. Furthermore, the within-group Bray–Curtis distances in the healthy group were significantly lower than those in the unhealthy group, suggesting increased microbial heterogeneity in the unhealthy oral environment (Supplemental Figure 1D).

Further subdividing the groups based on the effects of different orthodontic methods (Figures 1A, B) revealed that CAs could mitigate the increase in oral alpha diversity associated with unhealthy oral conditions. For example, the Shannon and ACE indices were significantly higher for CKH vs. CKU and FAH vs. FAU. However, no significant increase in these indices were found for CAH vs. CAU were found in the unhealthy group. Beta diversity analysis using PLS-DA revealed clear separation among groups, particularly for groups CKU, CAU, and FAU (Figure 1C). This result is consistent with the result of PCoA result (Supplemental Figure 2A, B), indicating distinct microbial community structures, especially in the context of an unhealthy oral environment. Interestingly, the within-group Bray–Curtis distances in group CAU were significantly lower than those in the other groups, suggesting that the CA group exhibited reduced microbial heterogeneity among individuals with unhealthy oral conditions (Figure 1D). Additionally, ANOSIM results (Supplemental Table 4) showed that oral health status ($R = 0.29$, $P = .001$) had a significantly greater effect on the oral microbiota than the type of orthodontic treatment ($R = 0.09$, $P = .001$).

Figure 1E shows the relative abundance of the top 10 dominant bacterial genera across groups, with key genera including *Streptococcus*, *Actinomyces*, *Leptotrichia*, *Veillonella*, and *Prevotella*. Notably, in groups CKU, CAU, and FAU, *Streptococcus* and *Actinomyces* decreased, whereas *Prevotella*, *Veillonella*, and *Leptotrichia* increased. Further LEfSe analysis (Supplemental Table 5) identified significantly enriched taxa in each group. *Lentimicrobium* was enriched in CKH. Meanwhile, among groups, CKU showed the highest number of enriched genera, including *Prevotella*, *Fusobacterium*, *Tannerella*, *Peptostreptococcus*, and *Treponema*. *Streptococcus* and *Granulicatella* were enriched in group C, *norank_f_norank_o_Clostridia_UCG-014* was enriched in group CAU, *Rothia* was enriched in group FAH, and *Anaeroglobus* was enriched in group FAU. Overall, these findings indicate that oral health status and orthodontic treatments significantly reshape the oral microbiota and lead to the enrichment of specific bacterial taxa.

Clinical factors are strongly correlated with oral microbiome variations and health-related habits

We performed RDA on genus-level species abundance data based on 10 collected clinical factors (Figure 2A) to evaluate the association between clinical factors and microbial community structure. The results revealed a significant separation between samples from healthy oral environment and unhealthy oral environment groups. Plaque index, the number of enamel demineralizations, and the number of

decayed teeth were all associated with the unhealthy oral environment groups, including CKU, CAU, and FAU. By contrast, factors such as gender, age, height, and weight, were associated with the healthy oral environment group. The long arrows representing plaque index, daily brushing frequency, and electric toothbrush use indicate the strong explanatory power for microbial community structure. Additionally, regression analysis (Figure 2B) revealed a significant positive correlation between plaque index and the first principal component (PC1) of PCA ($R^2 = 0.409$, $P < .01$).

Moreover, VPA (Figure 2C) revealed the interrelationships among "General," "Habit," and "OralMarker" and their contributions to the total variation. The overlap among these 3 factors accounted for a small proportion in the variation (2.7234%), with individual contributions of 3.3516% and 4.4304%. Notably, "OralMarker" alone contributed 7.2088% of the variation. The remaining 76.938% of residuals suggest that the majority of the variation is unexplained by these 3 factors, indicating the potential influence of other important factors on microbial community variation. Next, we performed Spearman correlation analysis between differentially abundant genera identified by LEfSe and clinical factors (Figure 2D). The results showed that the genera significantly enriched in the unhealthy oral environment group, such as *Prevotella*, *Tannerella*, *Centipeda*, *F0058*, *Treponema*, and *Lachnospiraceae* UCG-004, were positively correlated with the plaque index and lack of mouthwash use while being negatively correlated with daily brushing frequency. Conversely, genera that were significantly enriched in the healthy oral environment group, such as *Granulicatella*, *Streptococcus*, and *Rothia*, exhibited the opposite trends: They were negatively correlated with the plaque index and lack of mouthwash use but were positively correlated with daily brushing frequency. In summary, these findings suggest a significant association between changes in the oral microbiome and oral health status, as well as oral health-related habits.

Orthodontic treatment, especially treatment with CAs, significantly affects oral metabolites, particularly under compromised oral conditions

We conducted untargeted metabolomics analysis, detecting a total of 1977 metabolites, of which 832 were annotated in the KEGG database, to evaluate the effect of oral hygiene and orthodontic treatment on oral metabolites. sPLS-DA model analysis (Figures 3A–C) revealed significant separation of samples among groups, whether categorized by oral hygiene or orthodontic treatment, indicating a notable influence of both factors on metabolite composition. Interestingly, ANOSIM analysis (Supplemental Table 6) showed that, in contrast to the changes in the microbiome, the effect of oral hygiene on metabolites ($R = 0.113$) was smaller than that of orthodontic treatment (ANOSIM, $R = 0.182$), particularly under compromised oral conditions. Specifically, the differences between CKU vs. CAU ($R = 0.411$) and CKU vs. FAU ($R = 0.399$) were greater than those between CKH vs. CKU ($R = 0.379$), CAH vs. CAU ($R = 0.198$), and FAH vs. FAU ($R = 0.209$). Moreover, the effect of CAs on metabolites was greater than that of FAs, as shown by the larger differences between CKH vs. CAH ($R = 0.127$) compared with CKH vs. FAH ($R = 0.01$) and CKU vs.

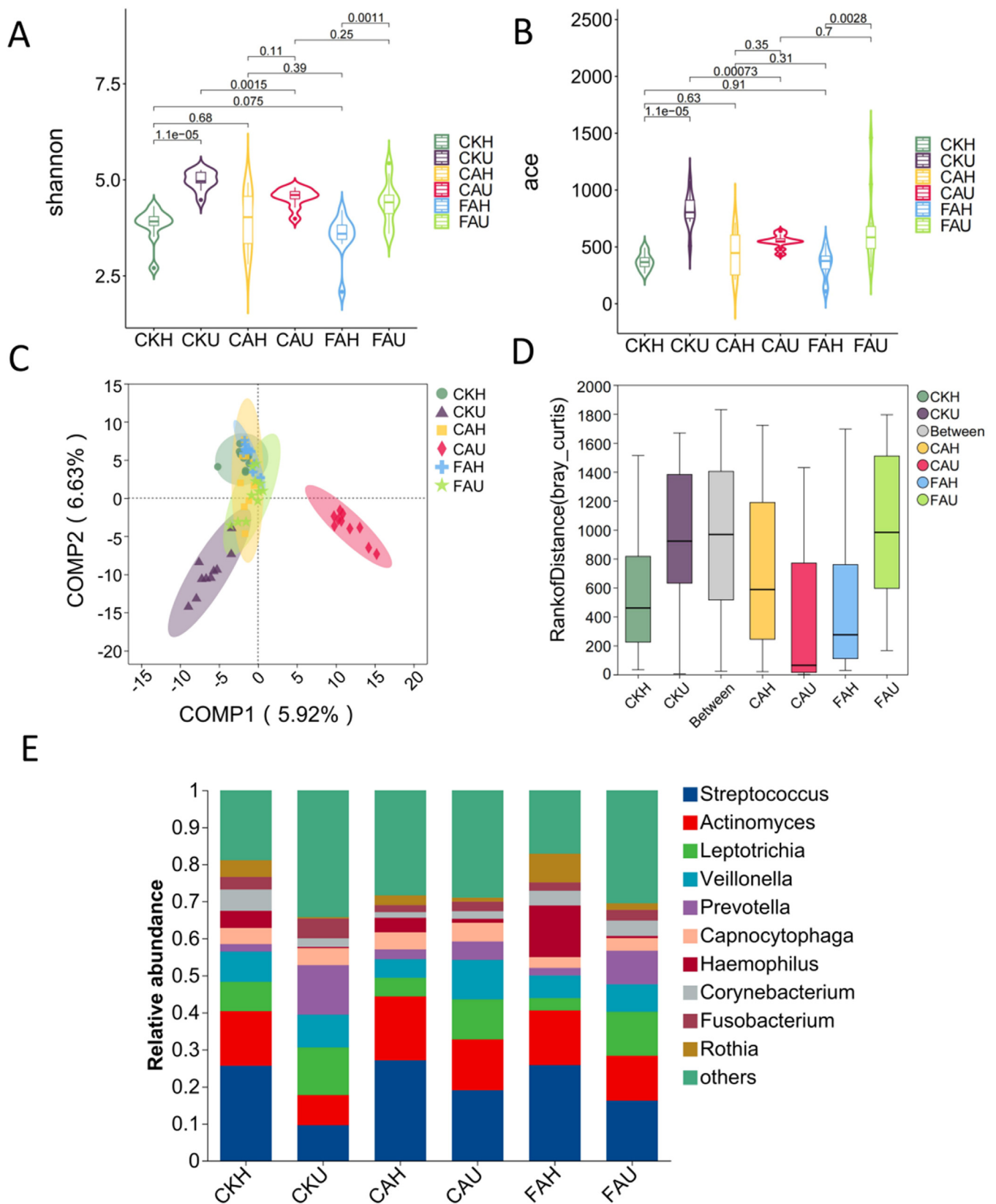


Fig. 1 – (A) Comparison of Shannon diversity index among different groups. (B) ACE richness estimator comparison among groups. (C) Partial least squares discriminant analysis (PLS-DA) of microbial communities across groups. (D) Box plot showing the rank of microbial Bray-Curtis distance across different groups. "Between" represents the distance between any 2 groups. (E) Stacked bar plot showing the relative abundance of the dominant Top10 bacterial genera across groups. The different colors represent various genera.

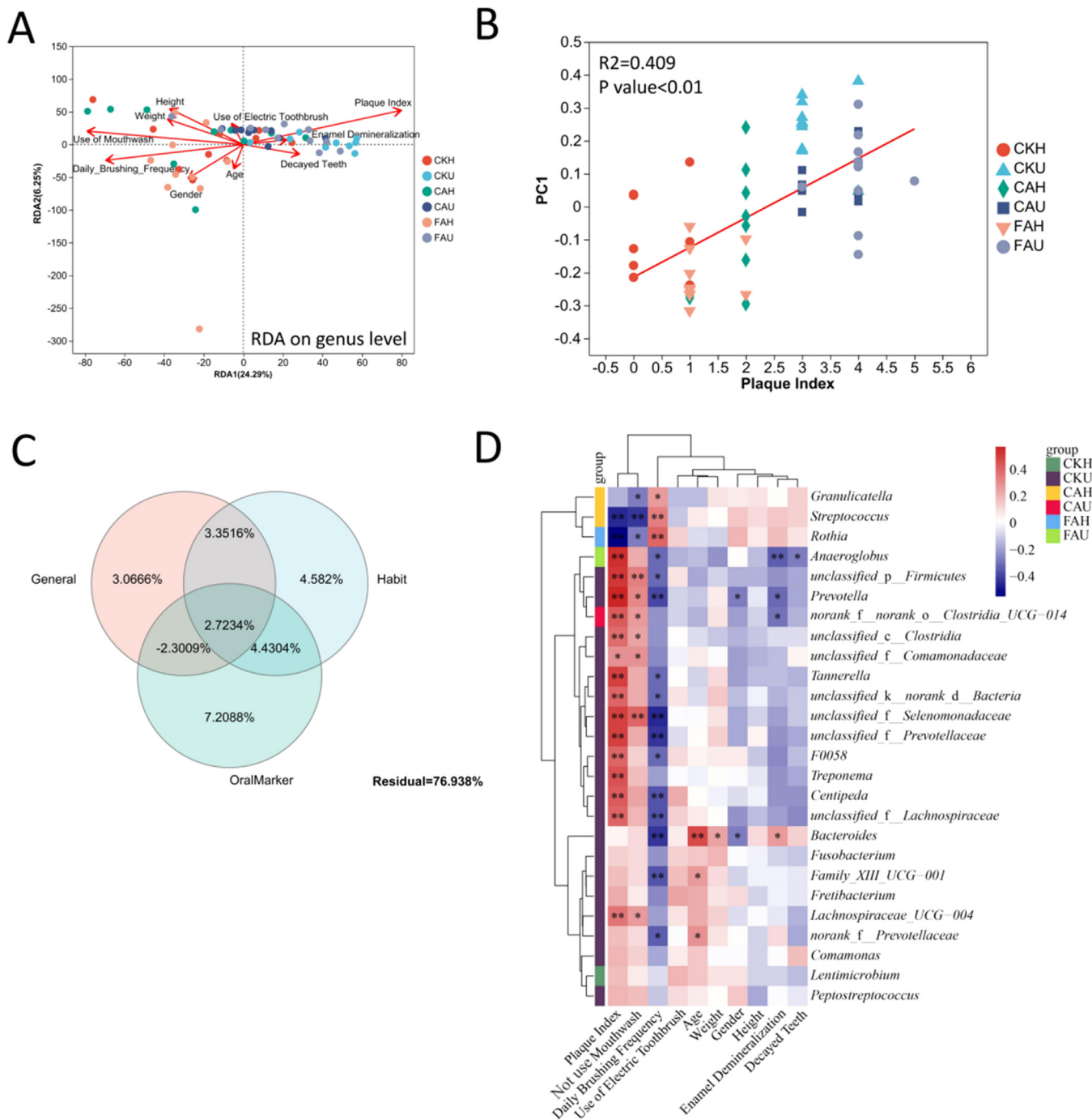


Fig. 2 – (A) Redundancy Analysis (RDA) at the Genus Level: The RDA biplot illustrates the relationships between various environmental variables (red vectors) and microbial communities at the genus level across different sample groups. Each point represents a sample, colored according to its group (CKH, CKU, CAH, CAU, FAH, FAU). The proximity of a sample to a vector indicates the extent of influence from that environmental factor. **(B) Correlation Between Plaque Index and Principal Component 1 (PC1):** The scatter plot shows the correlation between plaque index and PC1 scores derived from Principal Component Analysis (PCA) at the genus level. Different shapes and colors correspond to different sample groups, with a red regression line depicting the trend. The R-squared value of 0.409 and a p-value of less than 0.01 indicate a statistically significant correlation. **(C) Venn Diagram of Contribution Percentages Based on VPA Analysis at the genus level:** This diagram depicts the percentage contributions of 3 factors—General (4 demographic indicators: gender, age, height, and weight), Habit (3 lifestyle factors: daily brushing frequency, use of electric toothbrushes, and use of mouthwash), and Oral Marker (plaque index, enamel demineralization, and number of decayed teeth)—to the overall variation in the data. Overlaps between circles represent shared contributions among the factors, while the large residual percentage (76.938%) suggests a significant amount of unexplained variation. **(D) Heatmap of Differentially Abundant Genera Across Groups:** The heatmap displays the relative abundance of different genera, with the 'group' label indicating the genus enriched in the corresponding group as identified.

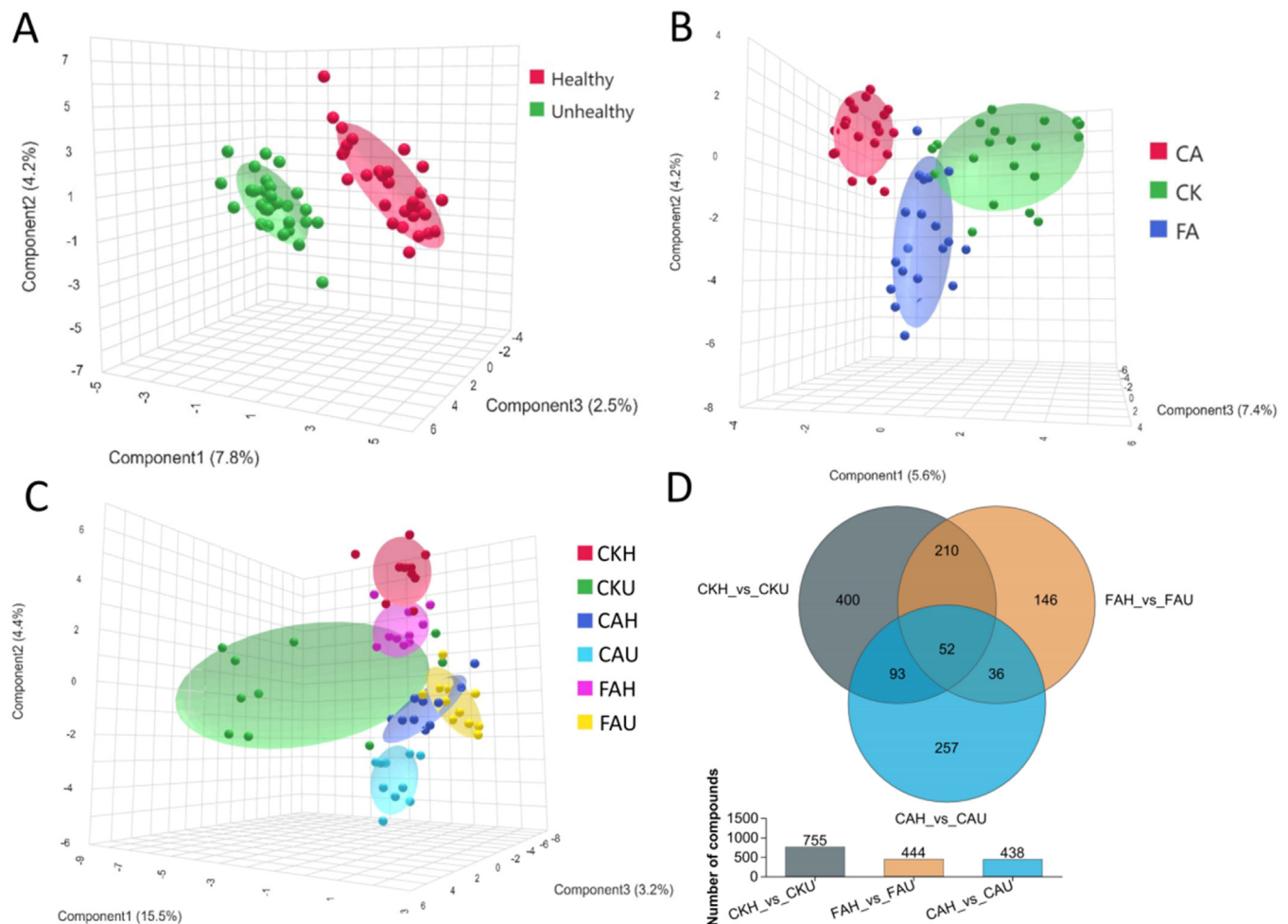


Fig. 3—(A) sPLS-DA analysis based on metabolite abundance in relation to oral health conditions. (B) sPLS-DA analysis based on metabolite abundance in relation to orthodontic methods. (C) sPLS-DA analysis based on metabolite abundance in relation to orthodontic methods and oral health conditions. (D) Venn comparison analysis of metabolites among different groups.

CAU ($R = 0.411$) compared with CKU vs. FAU ($R = 0.399$). These findings were consistent with the results from the metabolite Venn diagram analysis (Figure 3D), wherein the number of unique differential metabolites between CAH and CAU ($N = 257$) exceeded that between FAH and FAU ($N = 146$). A total of 616 metabolites with significant overall differences were identified by using PLS-DA with $VIP > 1$ and post hoc tests between groups ($FDR < 0.05$) (Supplemental Table 7) to further compare metabolite abundances across the 6 groups. KEGG enrichment analysis showed that these differential metabolites were enriched in pathways, such as map01064 (biosynthesis of alkaloids derived from ornithine, lysine, and nicotinic acid), map00785 (lipoic acid metabolism), and map01066 (biosynthesis of alkaloids derived from terpenoid and polyketide) (Table 2). Notably, pathway map01064

showed the most significant enrichment ($P = .0005$). This pathway, involving the biosynthesis of alkaloids from ornithine, lysine, and nicotinic acid, highlights ornithine as a key precursor in polyamine synthesis, which is crucial for bacterial replication, infection, and biofilm and dental plaque formation.^{19,20}

Identifying key metabolite signatures for predicting oral health using machine learning

We employed 3 machine learning models—LASSO, random forest, and SVM—to predict healthy and unhealthy states, to evaluate the predictive ability of oral metabolites for oral environmental health and identify key biomarkers under unhealthy oral conditions. The ROC curve results (Figure 4A)

by Lefse analysis (CKH, CKU, CAH, CAU, FAH, FAU). Colors range from red (high abundance) to blue (low abundance), with group classifications shown in the left sidebar. Significant differences in genus abundance between groups are marked with asterisks ($^*P < .05$, $^{**}P < .01$).

Table 2 – Analysis results of KEGG enrichment pathways for differential metabolites.

Pathway_id	Pathway description	First category	Second category	Enrich factor	Ratio_in_study	P_value
map01064	Biosynthesis of alkaloids derived from ornithine, lysine and nicotinic acid	Metabolism	Chemical structure transformation maps	0.67	18/154	.0005
map00785	Lipoic acid metabolism	Metabolism	Metabolism of cofactors and vitamins	1.00	6/154	.0017
map01066	Biosynthesis of alkaloids derived from terpenoid and polyketide	Metabolism	Chemical structure transformation maps	0.82	9/154	.0018
map04024	cAMP signaling pathway	Environmental Information Processing	Signal transduction	0.88	7/154	.0033
map00998	Biosynthesis of various antibiotics	Metabolism	Biosynthesis of other secondary metabolites	0.71	10/154	.0052
map00340	Histidine metabolism	Metabolism	Amino acid metabolism	0.69	11/154	.0053
map01070	Biosynthesis of plant hormones	Metabolism	Chemical structure transformation maps	0.63	12/154	.0097
map04922	Glucagon signaling pathway	Organismal Systems	Endocrine system	0.78	7/154	.0103
map00521	Streptomycin biosynthesis	Metabolism	Biosynthesis of other secondary metabolites	1.00	4/154	.0145
map04925	Aldosterone synthesis and secretion	Organismal Systems	Endocrine system	1.00	4/154	.0145
map00010	Glycolysis / Gluconeogenesis	Metabolism	Carbohydrate metabolism	1.00	4/154	.0145
map04072	Phospholipase D signaling pathway	Environmental Information Processing	Signal transduction	1.00	4/154	.0145
map01240	Biosynthesis of cofactors	Metabolism	Global and overview maps	0.51	21/154	.0182
map00280	Valine, leucine and isoleucine degradation	Metabolism	Amino acid metabolism	0.83	5/154	.0214
map04152	AMPK signaling pathway	Environmental Information Processing	Signal transduction	0.83	5/154	.0214
map05022	Pathways of neurodegeneration - multiple diseases	Human Diseases	Neurodegenerative disease	0.83	5/154	.0214
map01062	Biosynthesis of terpenoids and steroids	Metabolism	Chemical structure transformation maps	0.64	9/154	.0222
map00650	Butanoate metabolism	Metabolism	Carbohydrate metabolism	0.75	6/154	.0240
map01232	Nucleotide metabolism	Metabolism	Global and overview maps	0.54	14/154	.0327
map05032	Morphine addiction	Human Diseases	Substance dependence	1.00	3/154	.0420
map00900	Terpenoid backbone biosynthesis	Metabolism	Metabolism of terpenoids and polyketides	1.00	3/154	.0420
map05146	Amoebiasis	Human Diseases	Infectious disease: parasitic	1.00	3/154	.0420
map04068	FoxO signaling pathway	Environmental Information Processing	Signal transduction	1.00	3/154	.0420
map04911	Insulin secretion	Organismal Systems	Endocrine system	1.00	3/154	.0420
map04066	HIF-1 signaling pathway	Environmental Information Processing	Signal transduction	1.00	3/154	.0420
map04270	Vascular smooth muscle contraction	Organismal Systems	Circulatory system	1.00	3/154	.0420
map05014	Amyotrophic lateral sclerosis	Human Diseases	Neurodegenerative disease	1.00	3/154	.0420
map04540	Gap junction	Cellular Processes	Cellular community - eukaryotes	1.00	3/154	.0420
map04666	Fc gamma R-mediated phagocytosis	Organismal Systems	Immune system	1.00	3/154	.0420
map00760	Nicotinate and nicotinamide metabolism	Metabolism	Metabolism of cofactors and vitamins	0.64	7/154	.0474
map02020	Two-component system	Environmental Information Processing	Signal transduction	0.64	7/154	.0474

indicated that among the models, the LASSO model had the best classification performance (AUC = 0.9556), slightly outperforming random forest (AUC = 0.9545) and SVM (AUC = 0.9432). Additionally, LASSO identified 13 key metabolic features (Supplemental Table 8), which were grouped into 3 clusters on the basis of hierarchical clustering: subcluster 1 (N = 6), subcluster 2 (N = 5), and subcluster 3 (N = 2). Among these subclusters, subclusters 1 and 3 were upregulated in the unhealthy group, whereas subcluster 2 was downregulated in the unhealthy group (Figures 4B–D). Notably, the metabolite alpha-CEHC glucuronide (a vitamin E metabolite) in subcluster 2 was upregulated in the unhealthy oral environment. Under oxidative stress conditions, vitamin E is consumed rapidly, promoting the generation of its metabolites. Therefore, the upregulation of alpha-CEHC glucuronide might signal the oral tissue's response to oxidative damage.²¹ Figure 4E specifically illustrates the abundance changes of each metabolite across samples, showing a significant difference in distribution between the healthy and unhealthy groups. Furthermore, a Mantel test was conducted to examine the correlation among these 13 key metabolites and the microbiome at the genus level (Figure 4F). The results demonstrated a significant overall association between these metabolites and the microbiome ($R = 0.385$, $P = .001$, Supplemental Table 9). At the individual metabolite level, significant correlations were found for annomuricin B, LysoPE (15:0/0:0), and Zalypsin with the microbial community (Supplemental Table 8). The compounds 2-amino-4-hydroxy-6,7-dimethyl-5,6,7,8-tetrahydropteridine and 6-[4-(carboxymethyl) phenoxy]-3,4,5-trihydroxyoxane-2-carboxylic acid were significantly negatively correlated with the plaque index (Figures 4G–H), with R^2 values of 0.514 and 0.318, respectively. Conversely, LysoPE(15:0/0:0), cholestyramine, and alpha-CEHC glucuronide showed significant positive correlations with the plaque index (Figures 4I–K), with R^2 values of 0.34, 0.497, and 0.33, respectively. These findings further highlight the potential of these markers for monitoring oral health and the strong predictive power of the metabolome for determining oral health status.

Co-occurrence network analysis reveals complex interactions between oral microbes and key metabolites

First, Procrustes analysis (Supplemental Figure 3) demonstrated a significant overall correlation between the microbiome and metabolome based on all ASVs and metabolites ($P = .001$). Additionally, we conducted Procrustes and co-occurrence network analyses of differential genera and 616 differential metabolites (Supplemental table 10) to further elucidate the interaction mechanisms between oral microbes and metabolites. Co-occurrence network analysis (Figure 5) revealed a complex network comprising 163 nodes and 265 edges, with an average degree of 3.442. Key microbial hubs included F0058, *Peptostreptococcus*, *Prevotella*, *Rothia*, *Treponema*, and *Streptococcus*, which were associated with 54 salivary metabolites, 34 metabolites, 23 metabolites, 17 metabolites, 17 compounds, and 13 metabolites, respectively.

Salivary metabolites significantly associated with microbes included 41 organic acids and derivatives; 22 lipids and lipid-like molecules; 19 organoheterocyclic compounds;

10 nucleosides, nucleotides, and analogues; and 10 organic oxygen compounds. Among these salivary metabolites, key metabolites identified by the LASSO model included cholestyramine (metab_12922), which showed a significant negative correlation with *Rothia* (Spearman = -0.660 , $p = 7.17E-09$), and 2-hydroxypentanoic acid (metab_18131), which was significantly correlated with *Prevotella* (Spearman = 0.661 , $P = 6.74E-09$) and unclassified_f_Prevotellaceae (Spearman = 0.668 , $P = 4.06E-09$). Additionally, LysoPE (15:0/0:0) (metab_9682) exhibited a strong positive correlation with F0058 (Spearman = 0.611 , $P = 1.71E-07$), whereas alpha-CEHC glucuronide (metab_762) showed a significant positive correlation with *Anaeroglobus* (Spearman = 0.665 , $P = 4.89E-09$). Moreover, annomuricin B (metab_18984) was negatively correlated with *Prevotella* (Spearman = -0.606 , $P = 2.30E-07$) and positively correlated with *Rothia* (Spearman = 0.646 , $P = 1.92E-08$), indicating a close association between key metabolites and critical oral microbial genera. Furthermore, the core subnetwork identified through cytoHubba (Supplemental Figure 4) included the key microbial genera F0058, *Treponema*, *Streptococcus*, and *Prevotella*, as well as the key LASSO-identified metabolites 2-hydroxypentanoic acid (metab_18131), annomuricin B (metab_18984), and LysoPE (15:0/0:0) (metab_9682). These co-occurrence network analysis results revealed the intricate regulatory network between the oral microbiota and metabolites.

Discussion

In this study, we examined the effect of different orthodontic treatments and oral health conditions on health indicators, microbiota, and metabolomics. Participants were divided into 6 groups on the basis of oral environment (healthy vs. unhealthy) and treatment type (control, CAs, and FAs). By using plaque swabs, we assessed clinical factors, microbial diversity (16S rRNA sequencing), and metabolomics. Comparative and correlation analyses revealed several enriched microbiotas; metabolomics markers; and close relationships among orthodontic methods, oral health status, and microbial/metabolic changes (Supplemental Figure 5).

Orthodontic treatments, especially CAs, are linked to improved oral health outcomes. Oral health status and orthodontic methods significantly influence the oral microbiota. Consistent with a previous report,²² our present work found that in unhealthy environments, microbial diversity tends to increase, whereas CAs promote a more stable and balanced microbial community than FAs. Interestingly, the structure of the oral microbiota is more significantly influenced by the overall health of the oral environment than by the orthodontic treatment method. By contrast, the effect of orthodontic appliances on the oral metabolome structure is greater than that of oral health. The oral microbiota primarily reflects the microbial growth environment. In a healthy state, there is less plaque and few pathogens, leading to a relatively stable microbial community. Conversely, unhealthy conditions increase plaque accumulation and microbial diversity, making oral health status an important factor in microbiota structure. The metabolome reflects changes in biological processes, with orthodontic appliances affecting the physical

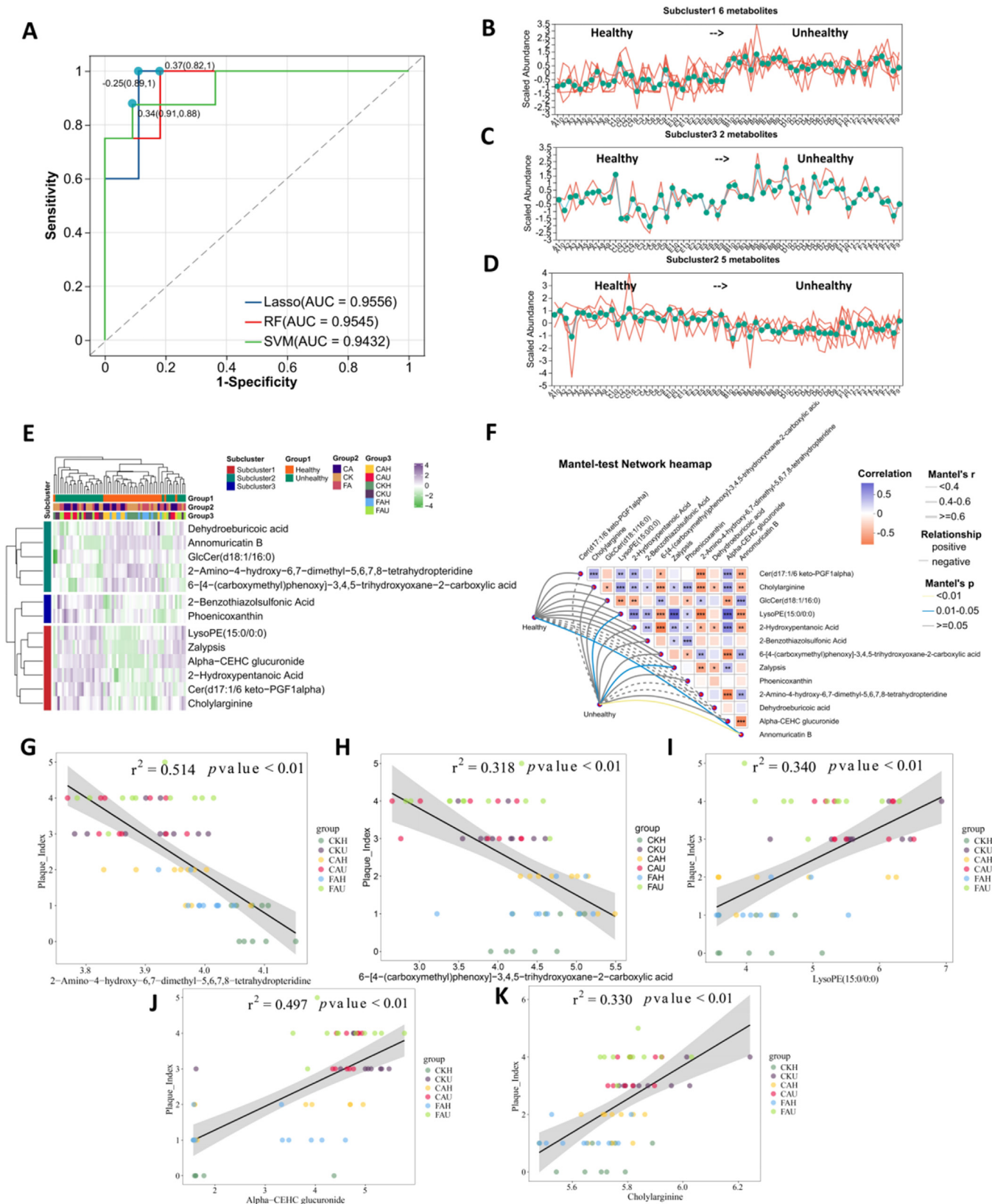


Fig. 4–(A) ROC curves of the 3 machine learning models. **(B–D)** Abundance changes of each subcluster in samples, based on hierarchical clustering; green dots represent the average abundance of each metabolite, and the lines represent individual metabolites. **(E)** Heatmap of key feature abundances selected by LASSO. **(F)** Results of the Mantel test between microbial genus level and LASSO-selected features. Spearman correlation coefficients were calculated between metabolites. **(G–K)** Regression analysis between specific metabolites and the Plaque Index. 2-Amino-4-hydroxy-6,7-dimethyl-5,6,7,8-

environment, such as saliva flow and food residue. This condition, in turn, substantially affects the production and accumulation of metabolites.

Machine learning models highlight the potential of oral metabolites as biomarkers for oral health. The LASSO model, in particular, demonstrates strong predictive performance, identifying 8 metabolites, including cholyarginine, Cer (d17:1/6 keto-PGF1alpha), 2-benzothiazolsulfonic acid, 2-hydroxypentanoic acid, LysoPE (15:0/0:0), alpha-CEHC glucuronide, phenicoxanthin, and Zalyopsis, that are upregulated in the unhealthy group, serving as key biomarkers indicative of poor oral health. Cholyarginine, in particular, is elevated in the unhealthy oral environment and potentially associated with oral microbiome imbalance and localized inflammatory responses. Poor oral health, such as periodontal disease, is often accompanied by chronic inflammation. During inflammation, tissue damage and immune cell activation may trigger the conjugation of amino acids, such as arginine, with bile acids, leading to the formation of cholyarginine. This process could represent a stress response to inflammation, explaining the upregulation of cholyarginine under such conditions.²³ Cer (d17:1/6 keto-PGF1alpha) is a specific type of sphingolipid (ceramide) conjugated with a prostaglandin, such as PGF1alpha, which is a key mediator in inflammatory responses. Prostaglandins play crucial roles in regulating vasodilation, immune cell recruitment, and pain perception during inflammation. Cer (d17:1/6 keto-PGF1alpha) may act as an inflammatory marker or regulatory factor that becomes upregulated in response to a localized inflammatory environment.²⁴ 2-Hydroxypentanoic acid (α -hydroxyvaleric acid) is an organic acid containing both hydroxyl and carboxyl groups. Poor oral health is often associated with the overgrowth of pathogenic bacteria, such as lactobacilli and streptococci, which can ferment carbohydrates and produce various organic acids, including 2-hydroxypentanoic acid. The increased metabolic activity of these bacteria can lead to the accumulation of these acidic byproducts, which are often linked to a decrease in oral pH and the demineralization of tooth enamel.²⁵ LysoPE (15:0/0:0) (lysophosphatidylethanolamine) is a type of lysophospholipid molecule. Unhealthy oral conditions, such as gingivitis and periodontitis, are typically accompanied by inflammation and tissue damage. This damage can lead to the breakdown of cell membrane phospholipids, resulting in the increased production of lysophospholipids like LysoPE (15:0/0:0). Phospholipids in cell membranes may be hydrolyzed by enzymes such as phospholipase A2 (PLA2) in response to inflammatory mediators or oxidative stress, thereby releasing lysophospholipids such as LysoPE.²⁶ Alpha-CEHC glucuronide (α -CEHC glucuronide) is a metabolite of vitamin E. Oxidative stress is a key mechanism underlying many oral diseases, such as gingivitis and periodontitis.⁵ In our study, alpha-CEHC glucuronide was found to be upregulated in unhealthy oral environments and identified as a key marker in the LASSO metabolite model for predicting oral health. Under conditions of oxidative stress, vitamin E is consumed more rapidly, leading to the increased production of its metabolites.²¹ Therefore, the upregulation of

alpha-CEHC glucuronide may serve as a signal of the oral tissue's response to oxidative damage. Further correlation analysis revealed a significant positive association between alpha-CEHC glucuronide and the enrichment of *Anaeroglobus* in group FAU. *Anaeroglobus* has been reported in the literature as a potential pathogenic bacterium strongly implicated in periodontitis.²⁷

Moreover, this study highlighted significant correlations between key metabolites and microbial genera, revealing intricate interactions within the oral microbiome. For instance, Cholyarginine shows a negative correlation with *Rothia*, whereas 2-hydroxypentanoic Acid had strong positive correlations with *Prevotella* and unclassified *Prevotellaceae*, suggesting their involvement in metabolic processes. LysoPE (15:0/0:0) and alpha-CEHC glucuronide were positively associated with F0058 and *Anaeroglobus*, respectively, indicating a link to inflammatory responses. Furthermore, anomuricin B's negative correlation with *Prevotella* and positive correlation with *Rothia* further demonstrate the complex regulatory network between metabolites and microbial activity in oral health. The close association between oral microorganisms and metabolism is closely related to the development and progression of host diseases. Another study investigated oral microorganisms and their metabolites in Type 2 Diabetes Mellitus (T2DM) patients without oral diseases. It found significant enrichment of periodontal pathogens, such as *Porphyromonas gingivalis* and increased levels of metabolites like cadaverine and L-(+)-leucine in T2DM patients compared with controls. These changes in the oral microbiome and metabolite profiles offer potential for developing oral biomarkers for the early detection of diseases beyond T2DM.²⁸

This study has several limitations that should be addressed in future research. First, the use of 16S rRNA sequencing for oral microbiome analysis did not permit precise species-level identification, thereby restricting the depth of functional gene analysis and exploration. Additionally, the metabolic markers identified in this study have not yet been validated through wet lab experiments, which are essential for confirming their biological relevance and accuracy. Furthermore, the sample size could be expanded in future studies to improve the reliability and generalizability of the results. Overcoming these limitations in subsequent research will enable a more comprehensive understanding of the oral microbiome and its metabolic functions.

This study offers a comprehensive look at how orthodontic treatments and oral health conditions affect microbial communities and metabolite profiles in the oral cavity. It highlights that clear aligners generally promote better oral health outcomes compared to FAs, especially in unhealthy environments. The findings suggest that while orthodontic treatments affect both the microbiome and metabolome, the overall health of the oral environment plays a more significant role in shaping microbial diversity. Machine learning models further emphasize the potential of certain metabolites as biomarkers for oral health, revealing intricate interactions between oral bacteria and metabolites. This detailed

tetrahydropteridine and 6-[4-(carboxymethyl)phenoxy]-3,4,5-trihydroxyoxane-2-carboxylic acid show significant negative correlations with the Plaque Index, with R^2 values of 0.514 and 0.318, respectively. LysoPE (15:0/0:0), cholyarginine, and Alpha-CEHC glucuronide show significant positive correlations with the Plaque Index, with R^2 values of 0.34, 0.497, and 0.33, respectively.

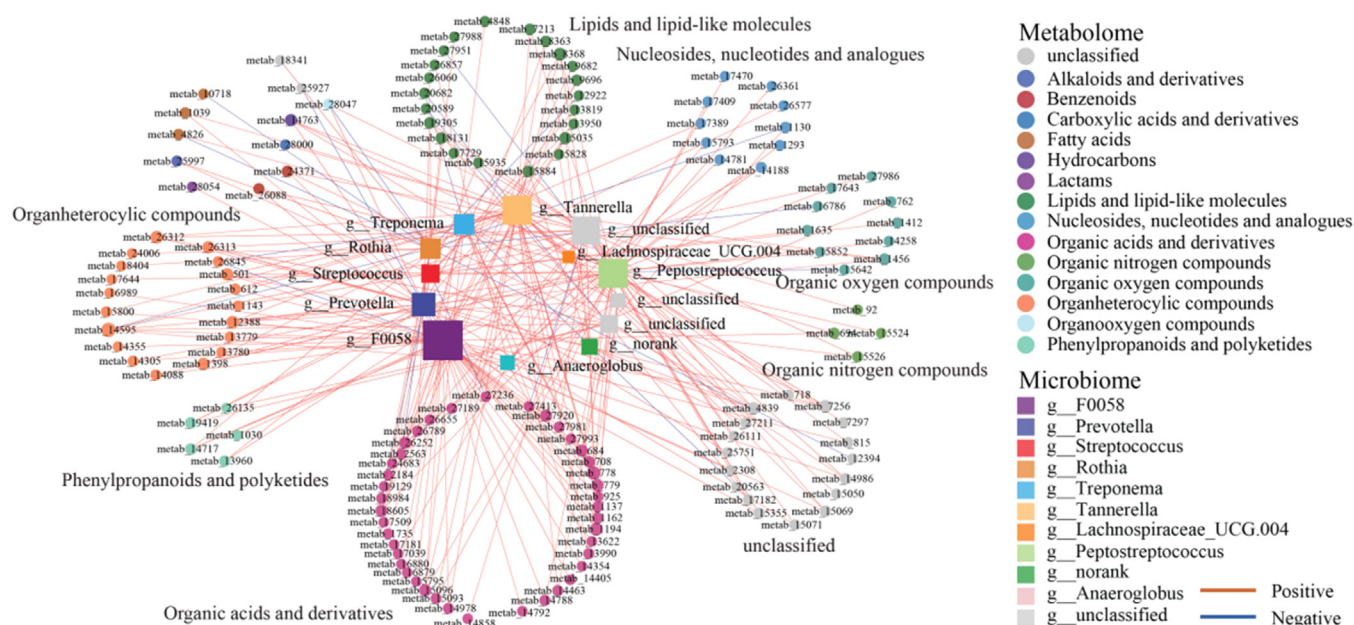


Fig. 5 – The network analysis illustrates the correlations between oral microbes and metabolites. Yellow solid lines indicate significantly strong positive linear relationships ($r \geq 0.6$, $P < .05$), while black dashed lines represent strong negative linear relationships ($r \leq -0.6$, $P < .05$). Blue lines depict significant nonlinear relationships. Circles correspond to metabolomics data, with different colors representing various metabolite superclasses, while squares represent microbiome data, with different colors indicating different taxonomic genera. The size of the circles and squares reflects their degree within the network.

analysis could guide future orthodontic practices and diagnostic approaches for managing oral health.

Conflict of interest

The authors declare that they have no known competing financial interests or personal relationships that could have appeared to influence the work reported in this paper.

Author contributions

Qin Xie: Conducting Experiment, Writing—original draft, Visualization, Validation, Software, Methodology, Investigation. Duo Li: Conception and Design of the study, Data curation, Conceptualization. Chengyan Ren: Visualization, Validation. Hao Liang: data collection. Weihui Chen: Writing—review and editing, Supervision, Project administration.

Funding

This work was supported by the Fujian Provincial Natural Science Foundation of China, Project No. 2023J01643.

Data availability

The raw amplicon sequencing data presented in this study can be found in NCBI Sequence Read Archive (SRA), and the accession number is PRJNA1149970. The metabolomics data

has been uploaded to the NGDC database, and the project number is PRJCA029433.

Code availability

The core software used is described in Materials and Methods. The scripts in this study are available on https://github.com/GoGoGao/orthodontic_microbiota.

Acknowledgments

We thanked Jianpeng Gao, Peng Wang and Xiaolun Cao for providing guidance on data analysis/writing during the preparation of this manuscript.

Supplementary materials

Supplementary material associated with this article can be found in the online version at [doi:10.1016/j.identj.2025.02.014](https://doi.org/10.1016/j.identj.2025.02.014).

REFERENCES

- Garcia RI, Henshaw MM, Krall EA. Relationship between periodontal disease and systemic health. *Periodontol* 2000 2001;25:21–36.
- Bui FQ, Almeida-Da-Silva CLC, Huynh B, et al. Association between periodontal pathogens and systemic disease. *Biomed J* 2019;42(1):27–35.

3. Altamura S, Del Pinto R, Pietropaoli D, et al. Oral health as a modifiable risk factor for cardiovascular diseases. *Trends Cardiovasc Med* 2024;34(4):267–75.
4. Jiang Q, Li J, Mei L, et al. Periodontal health during orthodontic treatment with clear aligners and fixed appliances: A meta-analysis. *J Am Dent Assoc* 2018;149(8):712–720.e12.
5. Shokeen B, Vilorio E, Duong E, et al. The impact of fixed orthodontic appliances and clear aligners on the oral microbiome and the association with clinical parameters: A longitudinal comparative study. *Am J Orthod Dentofacial Orthop* 2022;161(5):e475–85.
6. Crall, J.J. and C.B. Forrest, *A Life Course Health Development Perspective on Oral Health*, in *Handbook of Life Course Health Development*, N. Halfon, et al., Editors. 2018: Cham (CH). p. 299–320.
7. Rouzi M, Zhang X, Jiang Q, et al. Impact of clear aligners on oral health and oral microbiome during orthodontic treatment. *Int Dent J* 2023;73(5):603–11.
8. Rouzi M, Jiang Q, Zhang H, et al. Characteristics of oral microbiota and oral health in the patients treated with clear aligners: a prospective study. *Clin Oral Invest* 2023;27(11):6725–34.
9. Salminen A, Määttä AM, Mäntylä P, et al. Systemic metabolic signatures of oral diseases. *J Dent Res* 2024;103(1):13–21.
10. Liu B, Gao J, Liu XF, et al. Direct prediction of carbapenem resistance in *Pseudomonas aeruginosa* by whole genome sequencing and metagenomic sequencing. *J Clin Microbiol* 2023;61(11):e0061723.
11. Quigley GA, Hein JW. Comparative cleansing efficiency of manual and power brushing. *J Am Dent Assoc* 1962;65:26–9.
12. Chen S. Ultrafast one-pass FASTQ data preprocessing, quality control, and deduplication using fastp. *Imeta* 2023;2(2):e107.
13. Magoc T, Salzberg SL. FLASH: fast length adjustment of short reads to improve genome assemblies. *Bioinformatics* 2011;27(21):2957–63.
14. Callahan BJ, McMurdie PJ, Rosen MJ, et al. DADA2: High-resolution sample inference from Illumina amplicon data. *Nat Methods* 2016;13(7):581–3.
15. Bolyen E, Rideout JR, Dillon MR, et al. Reproducible, interactive, scalable and extensible microbiome data science using QIIME 2. *Nat Biotechnol* 2019;37(8):852–7.
16. Quast C, Pruesse E, Yilmaz P, et al. The SILVA ribosomal RNA gene database project: improved data processing and web-based tools. *Nucleic Acids Res* 2013;41(Database issue):D590–6.
17. Ren Y, Yu G, Shi C, et al. Majorbio cloud: a one-stop, comprehensive bioinformatic platform for multiomics analyses. *Imeta* 2022;1(2):e12.
18. Zhao Y, Zhu R, Xiao T, et al. Genetic variants in migraine: a field synopsis and systematic re-analysis of meta-analyses. *J Headache Pain* 2020;21(1):13.
19. Shah P, Swiatlo E. A multifaceted role for polyamines in bacterial pathogens. *Mol Microbiol* 2008;68(1):4–16.
20. Demkovych A, Kalashnikov D, Hasiuk P, et al. The influence of microbiota on the development and course of inflammatory diseases of periodontal tissues. *Front Oral Health* 2023;4:1237448.
21. Tothova L, Celec P. Oxidative Stress and Antioxidants in the Diagnosis and Therapy of Periodontitis. *Front Physiol* 2017;8:1055.
22. Zheng J, Wang X, Zhang T, et al. Comparative characterization of supragingival plaque microbiomes in malocclusion adult female patients undergoing orthodontic treatment with removable aligners or fixed appliances: a descriptive cross-sectional study. *Front Cell Infect Microbiol* 2024;14:1350181.
23. Ridlon JM, Harris SC, Bhowmik S, et al. Consequences of bile salt biotransformations by intestinal bacteria. *Gut Microbes* 2016;7(1):22–39.
24. Ricciotti E, FitzGerald GA. Prostaglandins and inflammation. *Arterioscler Thromb Vasc Biol* 2011;31(5):986–1000.
25. Featherstone JD. The science and practice of caries prevention. *J Am Dent Assoc* 2000;131(7):887–99.
26. Dennis EA. Diversity of group types, regulation, and function of phospholipase A2. *J Biol Chem* 1994;269(18):13057–60.
27. Griffen AL, Beall CJ, Campbell JH, et al. Distinct and complex bacterial profiles in human periodontitis and health revealed by 16S pyrosequencing. *ISME J* 2012;6(6):1176–85.
28. Li Y, Qian F, Cheng X, et al. Dysbiosis of oral microbiota and metabolite profiles associated with type 2 diabetes mellitus. *Microbiol Spectr* 2023;11(1):e0379622.